

See discussions, stats, and author profiles for this publication at: <https://www.researchgate.net/publication/230733359>

Studies of cavitation and ice nucleation in 'doubly-metastable' water: Time-lapse photography and neutron diffraction

ARTICLE *in* PHYSICAL CHEMISTRY CHEMICAL PHYSICS · AUGUST 2012

Impact Factor: 4.49 · DOI: 10.1039/c2cp41925d · Source: PubMed

CITATIONS

2

READS

28

5 AUTHORS, INCLUDING:



Phylip Rhodri Williams

Swansea University

130 PUBLICATIONS 859 CITATIONS

SEE PROFILE



Hoi Hong Chris Chan

Swansea University

9 PUBLICATIONS 14 CITATIONS

SEE PROFILE



M-C Bellissent-Funel

French National Centre for Scientific Resea...

196 PUBLICATIONS 4,872 CITATIONS

SEE PROFILE

Cite this: DOI: 10.1039/c2cp41925d

www.rsc.org/pccp

PAPER

Studies of cavitation and ice nucleation in ‘doubly-metastable’ water: time-lapse photography and neutron diffraction

Matthew S. Barrow,^a P. Rhodri Williams,^a Hoi-Houng Chan,^a John C. Dore^b and Marie-Claire Bellissent-Funel^c

Received 8th June 2012, Accepted 14th August 2012

DOI: 10.1039/c2cp41925d

High-speed photographic studies and neutron diffraction measurements have been made of water under tension in a Berthelot tube. Liquid water was cooled below the normal ice-nucleation temperature and was in a doubly-metastable state prior to a collapse of the liquid state. This transition was accompanied by an exothermic heat release corresponding with the rapid production of a solid phase nucleated by cavitation. Photographic techniques have been used to observe the phase transition over short time scales in which a solidification front is observed to propagate through the sample. Significantly, other images at a shorter time interval reveal the prior formation of cavitation bubbles at the beginning of the process. The ice-nucleation process is explained in terms of a mechanism involving hydrodynamically-induced changes in tension in supercooled water in the near vicinity of an expanding cavitation bubble. Previous explanations have attributed the nucleation of the solid phase to the production of high positive pressures. Corresponding results are presented which show the initial neutron diffraction pattern after ice-nucleation. The observed pattern does not exhibit the usual crystalline pattern of hexagonal ice [I_h] that is formed under ambient conditions, but indicates the presence of other ice forms. The composite features can be attributed to a mixture of amorphous ice, ice- I_h/I_c and the high-pressure form, ice-III, and the diffraction pattern continues to evolve over a time period of about an hour.

1 Introduction

Liquid water has been extensively studied in the normal liquid, supercooled liquid, supercritical liquid phases as well as in the disordered states corresponding to a range of amorphous ices that include hyper-quenched glassy water.^{1–6} The study of water under tension (or ‘negative pressure’) has not received the same attention due to the difficulty of producing stable samples, an early investigation being reported by Berthelot.⁷

This paper reports a study of cavitation in water in a ‘doubly-metastable’ state, being metastable with respect to both pressure and temperature. In the present work the term ‘doubly-metastable’ (d-m) refers to the liquid under tension below the normal ice-nucleation temperature. Herein, ‘nucleation’ refers to the inception of ice and reference to ‘cavitation nucleation’ is reserved for the rapid creation of gas/vapour cavities in the liquid.

It is interesting to speculate on the structure of the ice(s) which might form, even transiently, from supercooled water

under significant levels of tension. No structural information exists for ice formed from d-m water, or any other d-m liquid. Raman spectroscopy has been used to study ice-I formed from supercooled water⁸ and observations of the melting of metastable ice-I under tension have been reported,⁹ but in neither case was the ice formed from d-m water. To date, the formation of superheated ice from freezing superheated water has only been claimed for small positive pressures.¹⁰ The present molecular scale study employed neutron scattering techniques in order to examine the structural characteristics of ice formed in d-m water.

The Berthelot tube method

The Berthelot tube method exploits differences between the contraction of a container and its liquid contents to induce a state of hydrostatic, isotropic tension within the liquid (widely referred to as negative pressure).¹¹ Several studies of the method report work which involves sealing the tube with water and a small gas bubble, at a ‘sealing temperature’, T_s (point A in Fig. 1). The tube and sample are heated until the bubble disappears (at B) corresponding to the ‘filling temperature’, T_f . Thereafter, further heating causes the sample pressure to rise sharply (B–C), this pressurisation being reversed

^a College of Engineering, Swansea University, Swansea SA2 8PP, UK.
E-mail: m.s.barrow@swansea.ac.uk

^b School of Physical Sciences, University of Kent, Canterbury, CT2 7NH, UK

^c Laboratoire Léon Brillouin, C.E.A., Saclay, F-91191 Gif-sur-Yvette Cedex, France

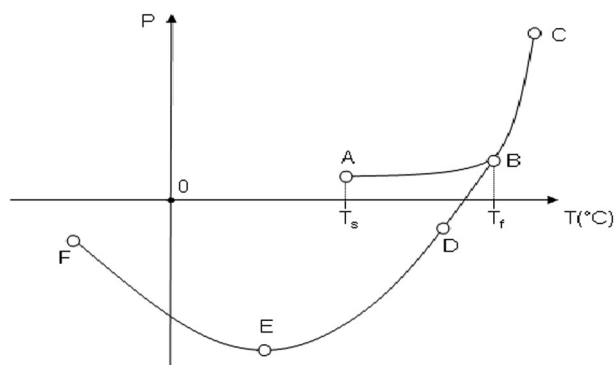


Fig. 1 Typical temperature–pressure profile of a Berthelot tube, illustrating sealing temperature T_s , filling temperature T_f and attainment of a d-m state prior to cavitation, e.g. point F.

on subsequent cooling. On cooling below T_f , the P–T profile diverges from the previous (heating) path as the bubble does not reappear and the liquid experiences tension as it attempts to contract within the confines of the tube (C–D). Thereafter, cooling of H_2O (or D_2O) produces a maximum tension at the temperature of maximum density, i.e. at point E (approximately 4 and 10 °C respectively). Thereon, further cooling reduces the tension, however net tension can be sustained below the normal nucleation temperature, such that the sample enters a d-m state. The tensile failure by cavitation (at point F) and the ensuing formation of ice is the subject of the current study.

Disparate values of the *breaking tensions* of water have been reported,^{12–14} the quantity of free and dissolved gas being considered particularly influential upon the results.^{15,16} Previous work has employed an initial bubble consisting either of air or water vapour, or mixtures of both, and the use of either degassed or aerated water. Depending on the composition of the gas and the initial bubble size, heating may substantially pressurise the liquid *prior* to the disappearance of the bubble (it has been suggested that the persistence of a gas bubble under high pressure is due to low values of diffusivity).¹⁴ A detailed description of an experimentally determined P–T profile is provided by Evans.¹⁷

Earlier investigations of doubly-metastable water

Hunt and Jackson¹⁸ studied the effect of cavitation in undercooled water which was superheated with respect to the vapour phase using a tension manometer and Henderson and Speedy^{19–21} reported the behaviour of water in the d-m region using a Bourdon–Berthelot tube. The latter results illustrate points of interest to the current study. They note that cavitation occurs when tensions reach a critical level, yet they also demonstrate that the maximum tension (at the point of maximum density) did not invoke cavitation in a water sample which subsequently cavitated under a lower tension in the d-m region.¹⁹ The cavitation event occurred overnight (presumably indicated by the observation of residual gas). The experiments were performed by first ‘dissolving’ an ‘air/water vapor bubble’. Other results reported include those for samples which neither cavitated nor exhibited the nucleation of ice in the d-m region. In all cases, ice nucleation was not observed.

In a later study, Henderson and Speedy report further results for H_2O and D_2O in the d-m region.^{20,21} Interestingly, given their previous observation, they note that ‘ice is always nucleated before the vapor phase in these experiments’.²⁰ Any interpretation of this statement should consider that their earlier observation (cavitation without nucleation)¹⁹ or later studies involving ‘cavitation when no ice was present’²¹ does not preclude the later formation of ice. Their later experiments also differed in that they used ‘substantially degassed’ water, thus either predominantly gaseous or vaporous cavitation can occur in their collected works.

Another excursion into the d-m regime was reported by Hayward,²² in whose work, water was held at -0.2 bar and -5 °C, which on further cooling froze to ice, while the intervening water ‘boiled’ at the same instant. However, in de-aerated water, ice appeared without relieving the state of tension. This latter observation is significant as it suggests that ice crystals may both form and grow in a liquid under tension. These conditions are different from those in which nucleation is accompanied by the relief of tension and the ice subsequently develops under ‘normal’ supercooled conditions at atmospheric pressure to form and grow as natural hexagonal ice (I_h).

2 Experimental

Berthelot tube design

In the present work the Berthelot tubes were evaluated in terms of their ability to sustain tension below the normal nucleation temperature and were designed to ensure compatibility with the neutron diffractometer test environment (in terms of materials and dimensions). The tubes were formed from straight silica glass tubes (internal diameter = 4.4 mm, wall thickness = 1.6 mm) sealed by a PTFE piston valve which allows outward flux of displaced liquid through the piston interior up to the point of sealing. The generation of tension within the sample acts to increase the integrity of the seal, however the valve is not designed for use at high positive pressure and this must be considered when pre-conditioning the liquid. The total length (tube and valve) was 120 mm, the sample-containing section of tube was 75 mm (see Fig. 2).

Sample preparation

The preparation of samples for the neutron diffraction study involved repeated cycles of pre-conditioning of D_2O (Sigma Aldrich, 99.9 atom% D) in a set of ten tubes. The purpose of this was twofold. Firstly, to ensure that the samples were sufficiently degassed, such that the tendency to ‘prematurely cavitate’ (herein, defined as cavitation at temperatures above 0 °C)

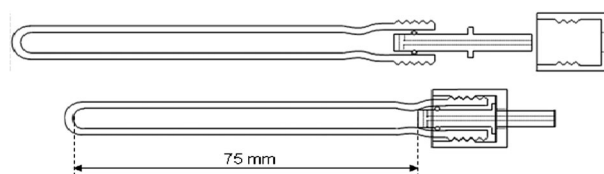


Fig. 2 Berthelot tube components, silica glass tube, piston (with embedded O-ring) and valve cap.

was reduced. Secondly, to identify individual tubes, sealing conditions and sample preparation methods which produced cavitation below the normal nucleation temperature. The tubes and samples were prepared and evaluated at the College of Engineering, Swansea, prior to despatch to the Laboratoire Léon Brillouin (L.L.B), C.E.A., Saclay. The method of evaluation was as follows.

Pre-conditioning of H_2O samples involved boiling prior to a secondary degassing under vacuum. In the case of D_2O , samples were sealed in the tubes and pressurised by heating to promote dissolution of very small gas bubbles which may not have been visible. The tubes were held vertically in a temperature controlled bath containing a solution of aqueous glycerol. The samples were allowed to achieve isothermal conditions with the valve held slightly above the bath surface to avoid contamination with glycerol.

The sample temperature was then reduced until cavitation occurred. Following cavitation, numerous bubbles persist within the liquid, these were collected and expelled by the addition of a small volume of fresh liquid. The process was repeated until the residual bubble volume diminished. A reduced tendency of the liquid to pre-cavitate resulted in some samples eventually cavitating below the normal nucleation temperature, thereafter the liquid froze. Thawing revealed numerous gas bubbles which were expelled and the process repeated until comparatively little gas was observed after thawing.

Further pre-conditioning experiments were performed by equilibrating the sample to the desired sealing temperature at ambient pressure. Thereafter, the valve was closed and the temperature raised until the residual bubble contracted, the tube being completely filled with liquid at T_f . Erroneous assessments of T_f can occur, as a reduction of the temperature at this point can result in the slow reappearance of the bubble in its original location. Accuracy was improved by focussing a fibre-optic light on the shrinking bubble, the persistence of a micro-bubble being indicated by a tiny reflective point. In any event, the temperature of the sample was raised still further to ensure that the liquid completely filled the tube.

Tubes were selected on the basis of their performance in experiments resulting in the production of ice in conjunction with an audible 'click' which signified cavitation. The occurrence of cavitation is the primary indication of a pre-existing tension; freezing without cavitation does not permit distinction between either a prior d-m state or supercooling in the absence of tension. After pre-conditioning, the selected tubes consistently produced ice without premature cavitation, however it was not possible to accurately predict the temperature at which cavitation accompanied by ice formation would occur. In general, this was not observed at temperatures greater than -5°C , most often it occurred around -10°C .

For the neutron measurements, pre-conditioned D_2O samples were subjected to several test runs before the samples were finally re-sealed at 19°C before raising to 40°C which was slightly above the perceived filling temperature. The samples were then cooled to ambient temperature and the tubes rinsed with water. The selected tubes were then sent to the Laboratoire Léon Brillouin (L.L.B), C.E.A., Saclay, for the neutron studies. On arrival the tubes were inspected and

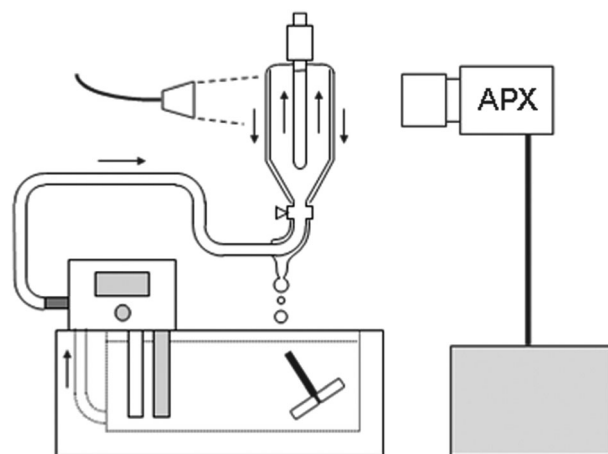


Fig. 3 External flow cell used for the photographic studies. Clamps and supports have been omitted for clarity.

did not contain any bubbles, confirming that the samples had not cavitating during transit.

High-speed photographic studies

Studies of the nucleation process used high-speed photographic techniques to record cavitation and ice formation. It was not possible to clearly observe samples inside the temperature controlled bath so an external circuit and flow cell was employed (see Fig. 3). The sample tube is clamped vertically and lowered into the open-topped cell. Coolant is pumped from the bath and through a valve at the base of the cell. The coolant fills the cell and overflows forming an exterior draining film which removes condensation and frost. High-speed, high-magnification photography required a high intensity light source, a fibre-optic light guide being employed. The camera was a 1-megapixel Ultima APX (Photron Europe Ltd, UK). The ice front velocity was measured using Sigmascan Pro 5.0 image analysis software (Systat Software Inc, UK).

The cavitation and ice propagation events imposed differing requirements in terms of frame rate, lighting (intensity and distribution) and magnification. The results shown in Fig. 4 and 5 show two different nucleation events (in two different tubes), Fig. 4 (high-magnification, high-speed) shows cavitation followed by ice-nucleation, Fig. 5 shows the propagation of ice within the Berthelot tube.

3 Results and discussion: photographic studies

The sequences shown in Fig. 4 and 5 clearly reveals that (i) the initial nucleation event corresponds to cavitation near the face of the piston and (ii) the first appearance of ice corresponds to the latter stages of cavitation activity. Thereafter ice propagates throughout the available sample volume. It is emphasised that ice formation is identified at the site of cavitation in the present experiments.

In Fig. 4, cavitation bubbles are seen to both grow and contract, *e.g.* between frames 3 and 4 and frames 6 and 7 respectively. Ice formation is recorded in frame 8, but it cannot be discounted that ice nuclei are present before this time. Significantly, frames 8 and 9 record a rebounding cavity in

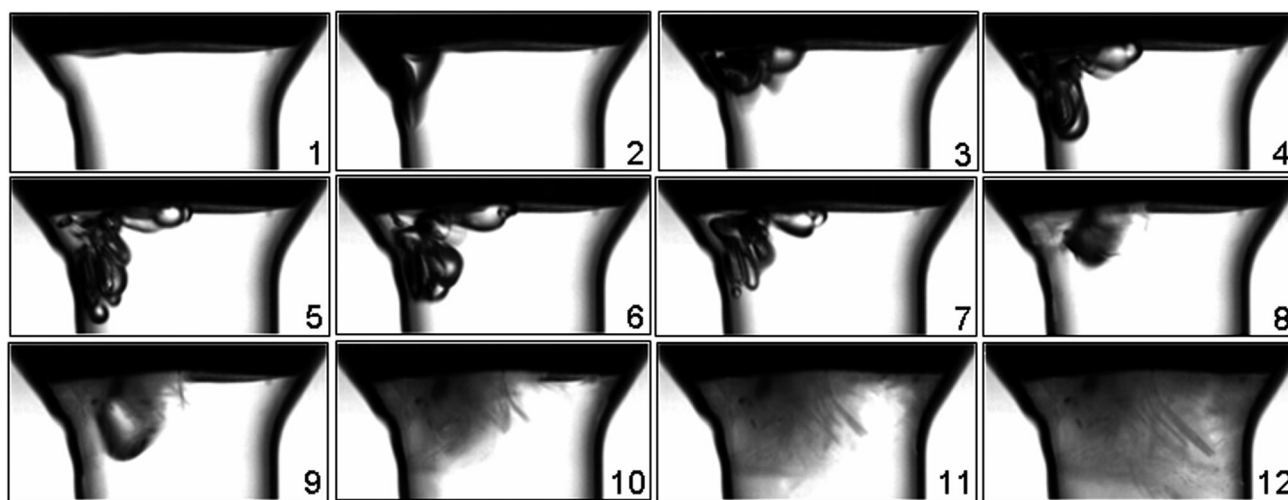


Fig. 4 High-magnification image sequence showing cavitation and ice-nucleation in the Berthelot tube. Water samples were substantially degassed, cavitation occurred at $-18\text{ }^{\circ}\text{C}$. Images were taken at 24 000 f.p.s. Frame-time reference (1 to 12, relative to frame #2) $-1.0, 0, 0.4, 0.7, 1.1, 1.4, 2.0, 5.2, 6.8, 12.0, 21.7$ and 76.6 ms.

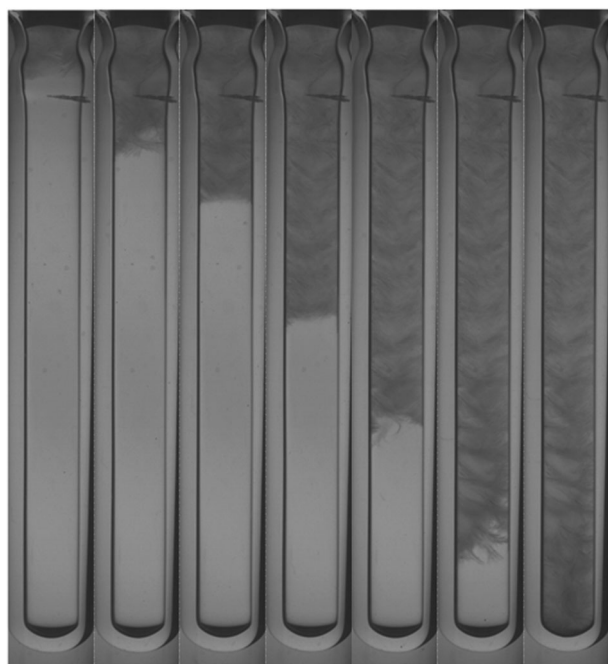


Fig. 5 Sequence showing the rapid formation of ice in a Berthelot tube. Frame-time reference (from left to right) $0, 112, 224, 512, 704, 848$ and 958 ms. Images were taken at 500 f.p.s.

immediate proximity to rapid ice formation. This cavity is obscured and enveloped by the solid phase; this illustrates that the gaseous phase may be quickly enveloped within the ice.

From time-referenced images, such as those shown in Fig. 5, the velocity of the advancing ice front can be measured. The speed appears to be dependent on the temperature, and the free-crystal growth rate is similar to that found in other studies.²³ The ice front speed increases with decreasing temperature (*e.g.* ice nucleated at -8 and $-12\text{ }^{\circ}\text{C}$ progressed through the sample at average speeds of 2.8 and 7.0 cm s^{-1} respectively).

An interesting feature shown in Fig. 5 is the appearance of band patterns, which suggest a repetitive feature in the

propagating front. These bands eventually disappear over tens of minutes, which is consistent with the time evolution observed in the neutron patterns (Section 4). The origin of the banded structure is not currently established but the darker bands may correspond to poly-crystalline ice and the lighter areas could suggest the presence of liquid or a glassy form of water/ice.

Needle-like ice structures originating near the wall of the tube suggest the formation of crystallites with specific orientations and preferred growth directions. The general characteristic appears to be the rapid growth of ice crystals, preferentially originating near the wall and conforming to the direction of ice propagation, *i.e.* if the tube is vertical, the ice needles appear to slant downwards describing an angle (with the wall) of between 50 and 70 degrees. The angle of the ice needles is subject to some variation between experiments (at different nucleation temperatures) although the general trend is consistent.

Factors influencing the degree of supercooling

Theories which describe the role of cavitation in ice nucleation typically invoke the collapse of a spherical bubble, in which situation it has been estimated that water near the bubble wall may experience sufficient pressure (10^4 bar) to nucleate a 'high pressure' form of ice.²⁴ Such pressures persist for only nanoseconds and it has been assumed that normal ice subsequently grows on a nanoscopic 'high pressure' ice nucleus. However, in order to generate sufficiently high pressures it is necessary to maintain sphericity of the bubble collapse event and this is unlikely. To date the existence of such a 'high pressure' ice nucleus has not been verified. The alternative explanation proposed herein involves the growth of a cavitation bubble in the supercooled liquid and the corresponding production of hydrodynamic pressures in a thin 'shell' of liquid close to the bubble wall.

The 'Rayleigh–Plessett' equation has been widely studied in terms of cavity collapse and the pressure generation in the surrounding liquid but herein we focus on the initial cavity

growth phase and the corresponding development of hydrodynamic pressures at various distances about the growing cavity. The hydrodynamic pressure p at a point r in the liquid in the neighbourhood of the bubble is given by the Bernoulli equation^{25,26}

$$p = \rho \frac{d\psi}{dt} - \frac{1}{2}(\rho v^2) + p_{\infty} \quad (1)$$

where p_{∞} is the pressure in the undisturbed water, ρ is the density and $v = -d\psi/dr$ is the radial velocity at that point, with velocity potential $\psi = (R^2/r)dR/dt$. The pressure variation Δp at r due to cavity motion is

$$\Delta p = p - p_{\infty} = \frac{\rho}{r} \frac{d}{dt} \left(R^2 \frac{dR}{dt} \right) - \frac{1}{2} \rho R^4 r^4 \left(\frac{dR}{dt} \right)^2 \quad (2)$$

Overton and Trevena²⁷ used the Bernoulli equation to account for the pressure–tension cycles recorded in their bubble oscillation experiments and in doing so associated the peak values of tension with the attainment of maximum cavity volume. When the cavity volume V reaches a maximum, d^2V/dt^2 is negative and this results in the development of tension due to the fact that, for values of r which are large enough to discount the second term in eqn (2), $d^2V/dt^2 \propto \Delta p$. Subsequent work established that the maximum negative values of d^2V/dt^2 (and hence the maximum tension) may precede the attainment of maximum cavity volume.^{28,29} From this it follows that a tension pulse is generated about a cavity during its growth phase. Due to the initial outward acceleration of the bubble wall, this liquid experiences a wave of positive pressure which reduces the degree of effective supercooling. Subsequently, as the bubble wall decelerates, the surrounding water is subjected to tension which increases the degree of effective supercooling and promotes a high probability of nucleation. As a result the bubble is encapsulated by a ‘shell’ of ice.

The recorded ice front speeds are commensurate with the velocities associated with the outward motion of the wall of a cavitation bubble wall during the latter stages of its expansion corresponding to the generation of tension within the liquid adjacent to the bubble wall.³⁰

Cavitation ultimately causes relaxation of the state of hydrostatic tension induced in the Berthelot tube technique but it is important to note that in the present case (involving both ‘cavitation nucleation’ and rapid ice formation), Fig. 4 shows that ice formation occurs *during* the cavitation event. This figure is one of a sequence showing cavity oscillation and, it follows from the theoretical explanation given above that if the cavity volume is still actively ‘cycling’ at the point of encapsulation then (dynamic) tension in the bulk liquid need not be released at the inception of ice formation.

The rapidity of ice formation in a Berthelot tube also presents novel conditions under which non-isothermal gradients may quickly appear as the exothermic formation of ice reduces the degree of the supercooling within the neighbouring liquid. A high rate of ice formation may then drive preferential nucleation at a distance further along the tube where the liquid maintains a reduced condition of supercooling. This in turn reduces the degree of supercooling in the next (and previous) section of the tube and the process is repeated along the entire length of the sample. The pressure within the warmer

interstitial sections then increases due to the formation and expansion of the ice bands, these ultimately freezing under a higher pressure as isothermal conditions are re-established. These arguments present reasonable grounds for a hypothesis that considers the co-creation of different ice forms from the liquid sample. In the following results section, a transiently changing neutron profile is reported for ice formed in a Berthelot tube.

4 Neutron diffraction studies

The neutron measurements reported herein were made on the 7C2 diffractometer at the Orphée reactor in the Laboratoire Léon Brillouin, C.E.A., Saclay. The sample tube was mounted in a closed-circuit refrigerator system at the centre of the diffractometer. It was found necessary to have good thermal contact with the copper blocks at both the top and the bottom of the tube. In this case, isothermal conditions cannot be fully established and a thermal gradient of approximately 2 °C was expected across the length of the tube. Measurements were made at fixed temperature increments, reducing from 20 °C to –15 °C. It was found necessary to run each sequential measurement for approximately five minutes to accumulate sufficient statistical accuracy in the diffraction profile. Data were also collected for an empty tube and standard corrections were applied to give the diffraction pattern for the water/ice as a function of temperature.

It was necessary to use D₂O instead of H₂O due to the high level of incoherent scattering from hydrogen. As the time-scale of the measurements needed to be short a high/medium-flux instrument was used. The results are discussed below.

The diffraction results for the first run are shown in Fig. 6 at various temperatures corresponding to the supercooled liquid and the initial ice phases immediately after nucleation.

There is a 10 minute increment between the data files for the a–f sequence and the final curve, g, corresponds to the stabilised ice phase formed more than two hours after the nucleation event. The results for the ‘stretched’ liquid state exhibit the expected behaviour in which the broad peak becomes displaced to lower Q -values as the temperature is reduced; these measurements will be reported separately. This feature is indicative of systematic changes in the hydrogen-bonding^{31,32} leading to increased connectivity and lower densities as the temperature is reduced.

The nucleation event in the first run occurred below –12 °C and gave an initial appearance of sharp Bragg peaks characteristic of ice, which varied continuously in intensity over the ensuing period of 60 minutes. Two thermocouples mounted on the top and bottom of the sample tube showed an exothermic heat flux at the time of the nucleation event. Because the thermometers are mounted remotely from the sample volume in the neutron beam, it is not possible to specify the temperatures for each of the diffraction patterns and it will be interesting to investigate the spatial distribution of the thermal changes in subsequent experiments. The overall characteristics of the low- Q peaks [$\sim 2 \text{ \AA}^{-1}$] in the diffraction pattern are similar to those corresponding to the structure factor for hexagonal ice [I_h], which displays a typical triplet profile, but the relative intensities of the peaks do not follow the predicted

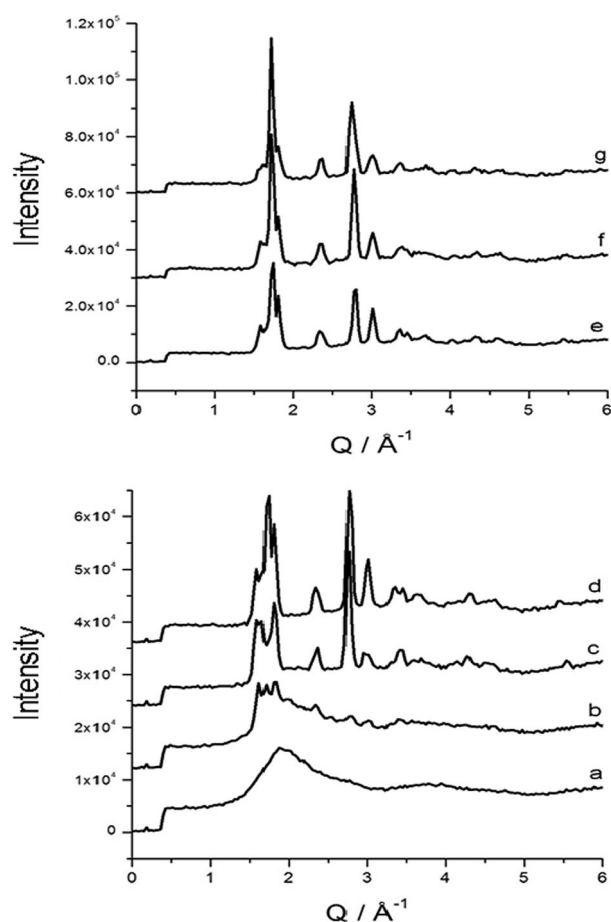


Fig. 6 Transient neutron diffraction spectra obtained for ice formed from doubly-metastable water. Following the time sequence a–g; the incremental time between data sets is 10 minutes; note the scale change from d to e. The data are normalised on a relative scale and plotted with a constant offset.

values and also change with time. Furthermore, there are two high intensity peaks at 2.75 and 3.05 \AA^{-1} that are not characteristic of ice-I.

Immediately after the nucleation event, the central peak [002] of the ice I_h triplet at $\sim 1.7 \text{ \AA}^{-1}$ is entirely absent but subsequently grows strongly to become the dominant peak at later times; there is also a corresponding loss of intensity for the two peaks at the higher Q -values. These features indicate that there are two distinct forms of crystalline ice present and that the relative amounts are changing with time. The high intensity peaks at $\sim 3 \text{ \AA}^{-1}$ are characteristic of Ice-III or Ice-IX, which are both high-pressure forms of ice. Since the starting temperature is ambient and heat is evolved, it is less likely that Ice-IX is present under these conditions, so the observed pattern suggests that ice-III is formed but subsequently some of this material transforms into ice-I. There is also a shift in the position of the peak at 2.8 \AA^{-1} that implies an increase in the lattice parameter due to the release of stress in the crystal. It is also apparent that the diffraction profile for ice-I changes and evolves over a period of about one hour stabilising after two hours. The growth of the main central peak of the triplet can be explained as an initial formation of a defective ice I_h in which the regular periodicity of the c -axis is

not well established and for which the subsequent increased intensity of the central peak indicates the later growth of cubic ice, I_c . It is well known from studies of ice nucleation in mesoporous silicas that a mixture of ice- I_h and ice- I_c is formed that is dependent on the pore size, filling factor, surface interaction and also varies with temperature, so the appearance of ice- I_c in these studies is not unexpected. The most extensive investigation of these features is covered in the paper by Webber and Dore³³ where references are given to other studies, such as Jelassi *et al.*³⁴

During these changes there is a corresponding reduction in the overall diffuse scattering level, indicating the conversion of a disordered form of ice, or possibly residual regions consisting of supercooled water, into one of the crystalline ice forms. It seems likely that this arises from the growth of the ice crystallites into regions of the sample that contain disordered ice or supercooled liquid.

Following the ‘annealing’ process, when the sample was heated towards ambient temperature, the overall scattering intensity was found to decrease. Removal of the Berthelot tube after the measurement revealed a small, localised failure of the tube. Consequently, the water/ice was exposed to the vacuum inside the chamber and evaporation of the liquid phase could occur as the sample was warmed. The thermocouple readings also exhibited increased variation, corresponding to fluctuations arising from the pumping of vapour from the sample. In a second run, nucleation occurred at a higher temperature of about -9°C as again indicated by a rapid increase in the thermocouple readings. No neutron data could be recorded in this case and at the end of the run it was found that the tube had fractured and the liquid contents dispersed.

5 Conclusions

The present results have indicated that studies can be made of the d-m state of water and its subsequent cavitation leading to transient ice formation. The time-lapse photography shows details of the initial cavitation event and the nucleation front within the sample. The neutron diffraction data indicate the structural changes that occur on a molecular scale, during and after the main event. The results provide information on a system that is far removed from the equilibrium states that are more usually studied and provides quantitative data for computational modelling of the cavitation dynamics. However, the possibility of investigating the short-time formation of the ice structure, immediately after cavitation, will require higher intensity radiation probes. These experiments might be feasible using synchrotron X-ray beams if appropriate sample cells could be produced for this situation and the doubly-metastable state can be preserved in a field of high-energy ionizing radiation. Further work is planned.

Acknowledgements

We wish to thank Professor Jack Powles for suggesting the current collaboration, Jean-Pierre Ambroise for technical support and Brigitte Beuneu for assistance during the neutron measurements. We also thank the EPSRC for their support and Thomas Loerting for helpful comments during the preparation of the paper.

References

- 1 O. Mishima and H. E. Stanley, *Nature*, 1998, **396**, 329.
- 2 M.-C. Bellissent-Funel, T. Tassaing, H. Zhao, D. Beysens, B. Guillot and Y. Guissani, *J. Chem. Phys.*, 1997, **107**, 2942.
- 3 J. L. Finney, A. Hallbrucker, I. Kohl, A. K. Soper and D. T. Brown, *Phys. Rev. Lett.*, 2002, **88**, 225503.
- 4 J. L. Finney, D. T. Brown, A. K. Soper, T. Loerting, E. Mayer and A. Hallbrucker, *Phys. Rev. Lett.*, 2002, **89**, 205503.
- 5 C. A. Tulk, C. J. Benmore, J. Urquidi, D. D. Klug, J. Neufeind, B. Tomberli and P. A. Egelstaff, *Science*, 2002, **297**, 1320.
- 6 A. Hallbrucker, E. Mayer, L. P. O'Mard, J. C. Dore and P. Chieux, *Phys. Lett. A*, 1991, **159**, 406.
- 7 M. Berthelot, *Ann. Chim. Phys.*, 1850, **30**, 232.
- 8 J. L. Green, A. R. Lacey and M. G. Sceats, *J. Phys. Chem.*, 1986, **90**, 3958.
- 9 E. Roedder, *Science*, 1967, **155**, 1413.
- 10 G. Schubert and R. E. Lingenfelter, *Science*, 1970, **168**, 469.
- 11 A. Imre and W. A. Van Hook, *Chem. Soc. Rev.*, 1998, **27**, 117.
- 12 H. H. Dixon, *Sci. Proc. R. Dublin Soc.*, 1909, **12**, 60.
- 13 R. S. Vincent and G. H. Simmonds, *Proc. Phys. Soc., London*, 1943, **55**, 376.
- 14 H. N. V. Temperley, *Proc. Phys. Soc., London*, 1946, **58**, 436.
- 15 G. D. N. Overton, M. J. Edwards and D. H. Trevena, *J. Phys. D: Appl. Phys.*, 1982, **15**, L129.
- 16 G. D. N. Overton, P. R. Williams and D. H. Trevena, *J. Phys. D: Appl. Phys.*, 1984, **17**, 979.
- 17 A. Evans, *J. Phys. E: Sci. Instrum.*, 1979, **12**, 276.
- 18 J. D. Hunt and K. A. Jackson, *J. Appl. Phys.*, 1964, **37**, 254.
- 19 S. J. Henderson and R. J. Speedy, *J. Phys. E: Sci. Instrum.*, 1980, **13**, 778.
- 20 S. J. Henderson and R. J. Speedy, *J. Phys. Chem.*, 1987, **91**, 3062.
- 21 S. J. Henderson and R. J. Speedy, *J. Phys. Chem.*, 1987, **91**, 3069.
- 22 A. T. J. Hayward, *Am. Sci.*, 1971, **59**, 434.
- 23 N. H. Fletcher, *The Chemical Physics of Ice*, Cambridge University Press, 1970, 115.
- 24 T. Inada, X. Zhang, A. Yabe and Y. Kozawa, *Int. J. Heat Mass Transfer*, 2001, **44**, 4523.
- 25 G. K. Batchelor, *An Introduction to fluid Mechanics*, Cambridge University Press, 1967.
- 26 H. N. V. Temperley and D. H. Trevena, *Liquids and their Properties: A Molecular and Macroscopic Treatise with Applications*, Ellis Horwood, Chichester, 1st edn, 1978.
- 27 G. D. N. Overton and D. H. Trevena, *J. Phys. D: Appl. Phys.*, 1981, **14**, 241.
- 28 P. R. Williams and P. M. Williams, *J. Phys. D: Appl. Phys.*, 1996, **29**, 1904.
- 29 P. R. Williams, P. M. Williams and S. W. J. Brown, *J. Phys. D: Appl. Phys.*, 1997, **30**, 1197.
- 30 M. S. Barrow, W. R. Bowen, N. Hilal, A. Al-Hussany, P. R. Williams, R. L. Williams and C. J. Wright, *Proc. R. Soc. A*, 2003, **459**, 2885.
- 31 M.-C. Bellissent-Funel, J. Teixeira, L. Bosio, J. C. Dore and P. Chieux, *Europhys. Lett.*, 1986, **2**, 241.
- 32 J. C. Dore, M. A. M. Sufi and M.-C. Bellissent-Funel, *Phys. Chem. Chem. Phys.*, 2000, **2**, 1599.
- 33 B. Webber and J. Dore, *J. Phys.: Condens. Matter*, 2004, **16**, S5449.
- 34 J. Jelassi, H. L. Castricum, M.-C. Bellissent-Funel, J. Dore, J. B. W. Webber and R. Sridi-Dorbez, *Phys. Chem. Chem. Phys.*, 2010, **12**, 2838.